Conf-910938--6

PNL-SA--19088

DE92 002146

PHASE STABILITY IN BE-NB AND BE-NB-ZR INTERMETALLICS

J. L. Brimhall
S. M. Bruemmer
L. A. Charlot

September 1991

Presented at the
International Conference on High
Temperature Intermetallics
September 16-19, 1991
San Diego, California

Work supported by
the U.S. Department of Energy
under Contract DE-AC06-76RLO 1830

Pacific Northwest Laboratory
Richland, Washington 99352

Abstract

Sputter deposition of Be-Nb alloys at low temperatures (30°C) produces an amorphous phase for compositions >5 at.% Nb. A metastable crystalline phase which can be considered a highly faulted form of the $Be_{12}Nb$ occurs at higher deposition temperatures or by low-temperature annealing of the amorphous phase. Because of structural similarities, this metastable phase is a precursor to the formation of either $Be_{12}Nb$ or $Be_{17}Nb_2$ upon high temperature annealing. There was no evidence of the Be_5Nb phase which has been postulated on some phase diagrams. The $Be_{12}Nb$ phase can accomodate considerable Zr in the structure and the $Be_{13}Zr$ can accommodate Nb into its structure. The $Be_{13}Zr$ becomes the predominant phase when the Zr/Nb composition ratio > 1. High temperature annealing of the ternary results in dual-phase regions of $Be_{12}(Nb,Zr)$ + $Be_{17}(NbZr)_2$ or $Be_{13}(Zr,Nb)$ + $Be_{17}(Zr,Nb)_2$, but the coexistence of $Be_{12}(Nb,Zr)$ + $Be_{13}(Zr,Nb)$ has not been observed.

I. Introduction

Refractory metal beryllides, $Be_{13}M$, $Be_{12}M$ and $Be_{17}M_2$, are currently of interest because of their potential high-temperature properties and very low density. As part of a larger program to evaluate deformation and fracture behavior in these beryllides, the phase relationships are also being studied. Phase relationships and phase stability are not firmly established in many of the beryllides. Some phase diagrams show only that certain phases exist but indicate nothing about the mode of transformation or thermal stability. A recently published Be-Nb phase diagram shows a high degree of uncertainly [1]. Knowledge of ternary relationships in these beryllides is practically non-existent. The purpose of the

present study was to evaluate the phase relationships and stability in the Be-Nb binary system and in the ternary Be-Nb-Zr. Recent studies [2]have shown that the phase relationship and stability between $Be_{12}M$ and $Be_{17}M_2$ may play a significant role in the deformation mode. It is of interest to know how ternary additons may affect this phase relationship.

II. Experimental Techniques

The alloys were prepared by high rate sputter deposition using specially designed targets to deposit a variable composition on the substrate. Figure 1 illustrates the different types of composite targets used. Targets having small disks of Nb or Zr resulted in a gradual composition gradient as opposed to strips of Nb (Fig. 1a) which resulted in a relatively steep concentration gradient. The composition was determined by EDX analysis in an SEM using a pure Nb standard. The analysis was checked against a cast alloy of $Be_{12}Nb$ for which the composition was known. Inductively coupled plasma (ICP) analysis was also used to corroborate the EDX measurements. Peak height ratios of the ternary alloy were analyzed by Auger spectroscopy (AES) to determine the concentration gradient.

Small sections several mm in size were cut from the deposit and the substrate removed by HNO_3. Annealing treatments were carried to 1100°C in argon or vacuum and times were typically one hour. Both diffractometer and Debye-Scherrer X-ray analysis were used. Some microstructural and electron

diffraction analyses were also obtained by transmission electron microscopy (TEM) on thinned sections.

III. Results

Binary Be-Nb Alloys

All binary alloys with compositions >5% Nb formed an amorphous structure when deposited at ambient temperatures. With compositions < 5% Nb, free Be was present in the deposit. Crystallization of this amorphous phase began about 500°C. The first phase to crystallize was a metastable form of $Be_{12}Nb$. The X-ray pattern is similar to that of $Be_{12}Nb$ but the first order (hk0) lines are missing. The pattern corresponds to a bcc structure with a_o=.521 nm, equal to $\sqrt{2}/2\ a_o$ of the $Be_{12}Nb$ phase. The patterns are shown in Table 1 for several different Nb compositions. This metastable phase, designated $Be_{12}Nb'$, appears to form at compositions extending up to at least 10% Nb. Also indicated in Table 1 is the Be pattern which is only observed for Nb concentrations <5 at.%.

This $Be_{12}Nb'$ phase was also identified in as-deposited material that was deposited at 400°C. No free Be was seen in this high temperature deposit until the composition dropped below about 5% Nb. At Nb compositions > 8%, an additional metastable phase designated X, was identified in the high temperature deposit. This phase could be indexed to a bcc structure with a lattice parameter of 1.208 nm, see Table 2. However, it did not fit any of the

known Nb beryllide phases nor any phases formed between Be and other refractory metals. This phase was only identified in the high temperature deposits and was not found in any of the annealed amorphous material.

Equilibrium phases began to appear upon annealing at temperatures ≥800°C. The $Be_{12}Nb$ phase (7.7 at.% Nb) was positively identified in the compositional range around 5-8%Nb. Annealing up to 1100°C failed to precipitate any free Be in deposits within a composition range from 5 to 7.7% Nb. If $Be_{12}Nb$ is a line compound, free Be should be present in this compositional range. X-ray patterns from material with >8% Nb indicated the $Be_{17}Nb_2$ phase, even though at lower annealing temperatures this composition showed the metastable $Be_{12}Nb'$ phase. The $Be_{12}Nb'$ phase is apparently a precursor phase to both $Be_{12}Nb$ and $Be_{17}Nb_2$. Reasons for this will be discussed. The metastable X phase was not observed after high temperature annealing and presumably transformed to the $Be_{17}Nb_2$ phase.

High temperature annealing of material with compositions >10.4% Nb produced a two-phase mixture of $Be_{17}Nb_2$ and Be_3Nb. Annealing at 1200°C for one hour produced no evidence of the Be_5Nb phase. Table 3 shows the pattern from a 14% Nb deposit, and all the lines can be accounted for by the $Be_{17}Nb_2$ and the Be_3Nb phases. The values given in Table 3 for Be_5Nb were taken from the pattern for Be_5Hf and reduced slightly to account for the smaller Nb atom. A phase with the composition of Be_5Nb has been reported [3] but there was no

crystallographic evidence presented.

The microstructure of the crystalline sputter deposited material was very fine grained as seen in the electron microscope, Figure 2. Analysis of the ring patterns from selected area diffraction patterns confirmed the x-ray analysis. However, it was not possible, due to the fineness and homogeneity of the structure, to isolate the individual phases.

Ternary Be-Nb-Zr Alloys

A variable composition Be-Nb-Zr deposit was made using the target configuration shown in Figure 1c. Substrate temperature was maintained at ~700°C for this deposit. Because of the high deposition temperature, a thin molybdenum layer was first put on the substrate to serve as a diffusion barrier between the beryllide and the copper substrate. The sum of the Nb+Zr composition was near 8 at.% and the compositional variation across the deposit is shown in Figure 3. At the center of the deposit, near the region of equal concentrations of Nb and Zr, there was a distinct change in appearance from metallic grey to black, which is also illustrated in Figure 3. This change is an optical effect due to changes in surface topography but is also indicative of microstructural and/or phase changes.

X-ray analysis of the as-deposited structure in the high Nb region of the deposit showed a mixture of the metastable $Be_{12}Nb'$ phase and the unknown X phase,

Table 4. The lines from the $Be_{12}Nb'$ were more intense indicating a greater concentration of this phase. The pattern was similar to that seen in the binary alloy deposited at 400°C with 8-10 at% Nb. This X-ray pattern persisted with increasing Zr until the Zr concentration was greater than the Nb concentration which coincided with the change in surface appearance. The pattern from region B of Figure 3 also showed a very strong texture in the $Be_{12}Nb'$ phase. The X-ray pattern of the dark region where the Zr/Nb > 1 indicated only the $Be_{13}Zr$ phase, Table 4. There was no evidence of any $Be_{12}Nb$ phase or $Be_{17}(Nb,Zr)_2$ phase in the patterns from the region of higher Zr concentration.

Consistent with the binary alloy, the $Be_{12}(Nb,Zr)'$ and the unknown X phase in the ternary alloy transformed to the $Be_{12}M$ or $Be_{17}M_2$ type phases after annealing at 1000°C. A two phase region of $Be_{12}(Nb,Zr)$ + $Be_{17}(Nb,Zr)_2$ was observed in the high Nb region of the deposit (A to B in Figure 3). The strong texture from region B was still present and identified as the (002) plane of the $Be_{12}Nb$ parallel to the plane of the deposit. In the high Zr side of the deposit (C in Figure 3), a two phase region of $Be_{13}(Zr,Nb)$ + $Be_{17}(Zr,Nb)_2$ was observed after annealing. Within the limits of the analysis, no two phase region of $Be_{12}(Nb,Zr)$ + $Be_{13}(Zr,Nb)$ has been observed in the annealed deposits.

IV. Discussion

Several metastable phases are formed in the refractory metal beryllide systems

during sputter deposition. The amorphous phase has been formed in many different intermetallic systems as a result of very rapid liquid or gas phase quenching [4-7]. The amorphous phase can form at Nb concentrations down to about 4 to 5 at.%. This limit coincides with the lower concentration limit observed for the $Be_{12}Nb$ phase and suggests that the formation of the amorphous phase at low deposition temperature is closely related to the formation of an intermetallic compound at high temperatures.

In the formation of crystalline phases during sputter deposition a high degree of faulting of the structure can be expected. Banerjee et.al [8] have shown how faulting in cast $Be_{12}Nb$ can produce the $Be_{17}Nb_2$ structure. Such a transformation is illustrated in Figure 4. A similar type transformation has been proposed by Bruemmer, et. al. [2] to describe deformation processses in $Be_{12}Nb$. The ease of transformation from one structure to the other has also been demonstrated in some ternary rare earth compounds [9].

Heavy faulting can also explain the metastable $Be_{12}Nb'$ phase. An (001) projection of perfect and faulted structures is shown in Figure 5. It can be seen that a very high density of faults will place atoms in positions that effectively eliminate the (110) planes and the first X-ray reflection of the (hk0) type would occur from the (220) planes as demonstrated in Figure 5b. The same reasoning would apply to other first order (hk0) planes. Because of this heavy faulting of $Be_{12}Nb$, the $Be_{12}Nb'$ can be considered a precursor phase to either $Be_{12}Nb$ or $Be_{17}Nb_2$.

In the ternary deposit, both the $Be_{12}Nb$ and $Be_{13}Zr$ can accommodate the other refractory metal element into its structure. The analysis does not allow precise limits on solubility but it is significant, e.g. up to 30% of the Nb sites could be occupied by Zr atoms. It appears that one or the other of the phases is preferred during sputter deposition of the ternary depending on the ratio of Nb/Zr. This is probably due to the lack of a structural relationship between the $Be_{13}M$ and the $Be_{12}M$ phases as there is between the $Be_{12}M$ and the $Be_{17}M_2$. The formation of the phases depends strongly on the size of the M atom, with small atoms preferring the $Be_{12}M$ structure [10]. The $Be_{12}(Nb,Zr)$ phase will be stable and accommodate Zr atoms until the average size of the Nb+Zr atom reaches a critical value at which point the $Be_{13}(Zr,Nb)$ phase becomes stable.

V. Acknowledgments

This work was supported by the Defense Advanced Research Projects Agency through the Office of Naval Research and the U.S. Department of Energy under Contract DE-AC06-76RLO 1830 with Pacific Northwest Laboratory which is operated by Battelle Memorial Institute.

VI. References

1. Binary Alloy Phase Diagrams, ed. by T. B. Massalski, ASM International, Metals Park, OH, 1990 edition.
2. S. M. Bruemmer, L. A. Charlot, J. L. Brimhall, C. H. Henager, Jr. and J. P. Hirth, "Dislocation Structures in Be12Nb after High-Temperature

Deformation", submitted to Phil. Mag.

3. P. M. Arzhanyi, R. M. Volkova and D. A. Prokoshkin, Proc. Acad. Sci. USSR, 150, (1963) 388.

4. J. L. Brimhall, H. E. Kissinger and R. Wang, J. Mat. Sci., 16, (1981) 994.

5. L. E. Tanner and R. Ray, Acta Met., 27, (1979) 1727.

6. H. F. Rizzo, L. E. Tanner, M. A. Mall, E. D. McClanahan and T. B. Massalski, in "Fundamentals of Beam Solid Interactions and Transient Thermal Processing", MRS, Pittsburgh, PA, (1988) 81.

7. T. W. Barbee Jr. and D. L. Keith in E. S. Machlin and T. J. Rowland eds., "Synthesis and Properties of Metastable Phases", TMS Warrendale, PA, (1980) 93.

8. D. Banerjee, L. Jacobson, J. Zindell and T. E. Mitchell in L. A. Johnson, D. P. Pope and J. O. Stiegler eds., High Temperature Ordered Intermetallics IV, MRS, Pittsburgh, PA, (1991) 397.

9. I. Felner, J. Less Common Metals, 72, (1980) 241.

10. G. V. Raynor, in Proc. of the 4th Intl. Conf. on Beryllium, The Metals Society, London (1977) 2/1.

Table I. Observed d-Spacings from Amorphous Be-Nb Deposits Annealed at 650 - 750°C

Observed d-spacings			Calculated	Card File			
3.5%Nb	5.5%Nb	9.0%Nb	bcc(a_o=.521)	$Be_{12}Nb$	(hkl)	Be	(hkl)
				.520	(110)		
.3668	.369	.3679	.3676 (110)	.369	(101)(200)		
.2603	.262	.2591	.2600 (200)	.2608	(211)(220)		
				.2327	(310)		
.214	.213	.2145	.2123 (211)	.2127	(002)(301)		
				.1971	(112)	.197	(100)
.1975*							
.1833	.185	.1844	.1839 (220)	.1842	(202)(402)	.179	(002)
.1797							
				.1736	(330)	.173	(110)
.1730							
	.1661	.1649	.1644 (310)	.1648	(222)(411)(420)		
				.1573	(312)		
				.1445	(510)		
	.1402	.1395	.1390 (321)	.1393	(103)(402)		
				.1344		.133	(102)
		.1306	.1300 (400)	.1302	(213)(422)		
	.1278		.1226 (411)	.1226			

*Bold figures indicate Be lines

Table II. Comparison of d-Spacings of the Unknown Phase (X) with Calculated bcc Pattern, a_o = 1.208 nm

Measured Values	(Int.)	Calculated Values	(hkl)
.4912	(34)	.4927	(211)
.4263	(42)	.4267	(220)
.3811	(100)	.3816	(310)
.367*		-	-
.3510	(<3)	.3484	(222)
.3219	(40)	.3225	(321)
.3025	(<3)	.3017	(400)
	-	.2845	(411)
	-	.2699	(420)
.2571*	(38)	.2573	(332)
.2464	(21)	.2463	(422)
.2367	(94)	.2367	(431)(510)
.2279	(72)	-	-
.2206	(38)	.2204	(521)
.2121*	26)	.2133	(440)
-		.2069	(433)
-		.2012	(442)(600)
.1960	(71)	.1958	(532)
.1911	(54)	.19084	(620)
.1863	(55)	.1862	(541)
.1840*		-	-
-		.1819	(622)
.1781	(12)	.1780	(631)
.1743	(9)	.1742	(444)
.1706	(6)	.1707	(550)(710)
-		.1674	(640)
.1645	(26)	.16425	(552)
.1615	(14)	.1613	(642)

* $Be_{12}Nb$' lines

Table III. Comparison of the Observed d-Spacings from 14% Nb Alloy, Annealed at 1200°C for One Hour, with X-ray Card File Values

Observed Values	$Be_{17}Nb_2$	Be_3Nb	Be_5Nb (Est. from Be_5Hf)
.7021		.702	
.5527	.550		
.4130	.414		
.3877		.388	
			.382
.3698	.370	.370	
.3556	.362	.351	
			.342
.3077	.308		
.2768	.276		
.2578	.259		
			.253
.2490	.250		
.2383	.237	.239	
.2287		.228	
			.223
.2208	.221		
.2142	.214		
.2065	.206		
.1972		.197	
			.194
.1919		.191	
.1848	.185		
.1803	.180		

Table IV. Measured d-spacings from Be-Nb-Zr Deposit for Different Nb/Zr Concentration Ratios

Region (see Figure 3)				
(A)	(B)	(C)	(D)	$Be_{13}Zr$ (Card File)
		.5027	.503	.504
.4893	.497			
.4253				
.3814	.384			
.3661*	.370*			
.3220		.3552	.3551	.354
		.2897	.2895	.289
.2594*	.2604*			
.2461		.2512	.2517	.251
.2367	.238		.2327	
.2206				.224
.2116*	.2138*	.2047	.2049	.2045
.1961				
.1912				
.1863				
.1837*	.185*			
.1782		.1773	.1773	.1775
.1745	.175			
.1710				.1700
.1644*		.1669	.1674	.1673
.1615				
.1587		.1584	.1590	.1585
.1536				
.1511		.1511	.1515	.1514
.1500				
.1480				

*$Be_{12}Nb$' lines

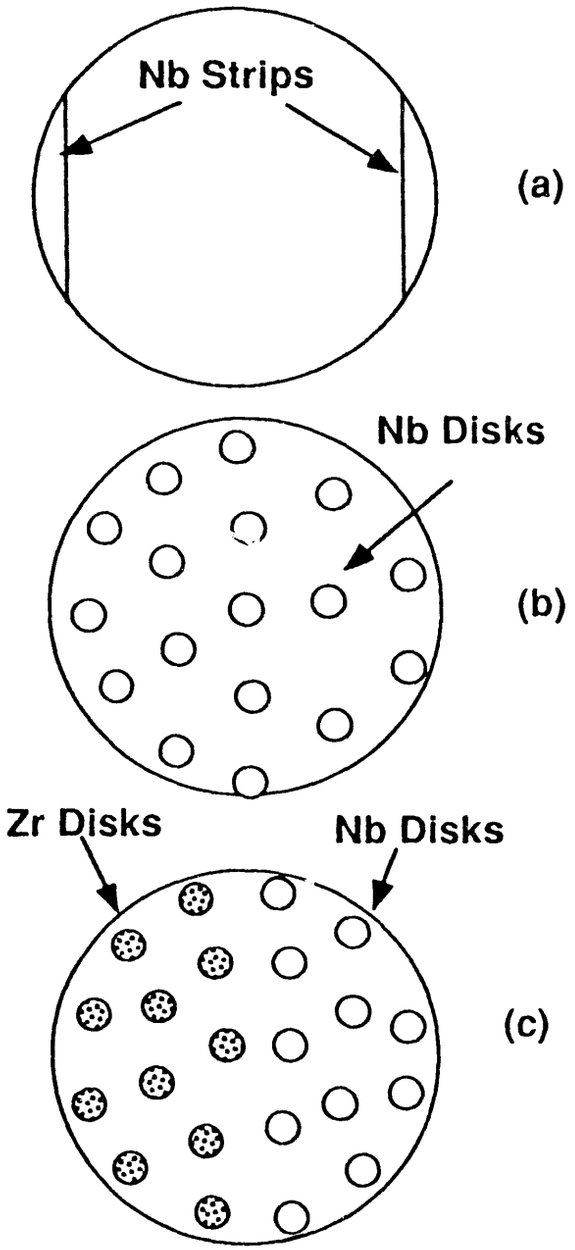

Figure 1. Target configurations used to get variable composition in the deposit. (a) Steep concentration gradient with Nb minimum in center. (b) Gradual concentration gradient. (c) Variable concentration gradient of Zr and Nb. Sum of Nb+Zr is constant.

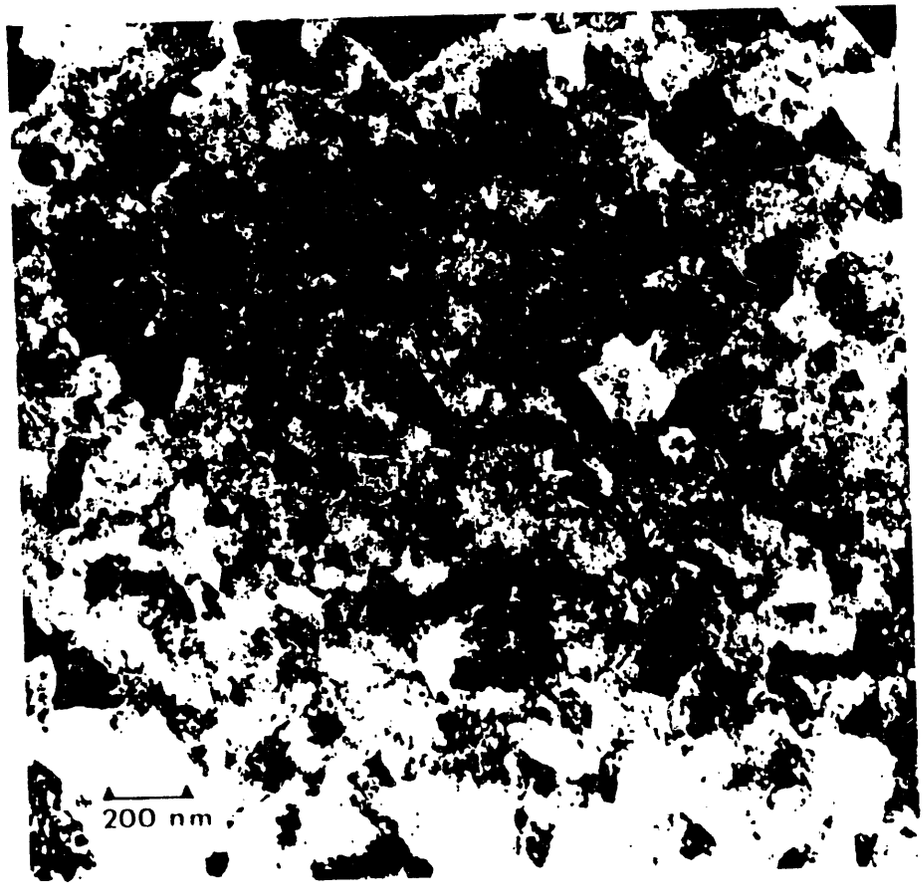

Figure 2. Electron micrograph of Be-5%Nb alloy, sputter-deposited at room temperature and annealed at 650°C for one hour.

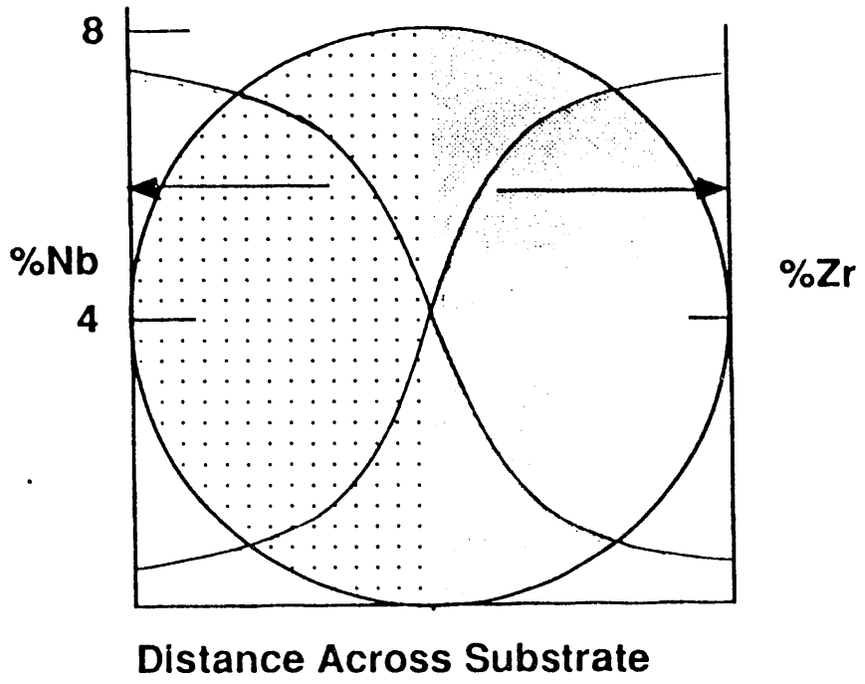

Figure 3. Schematic of concentration gradient across the Be-Nb-Zr deposit. Contrast change in the deposit occurs at about equal concentrations of Nb and Zr.

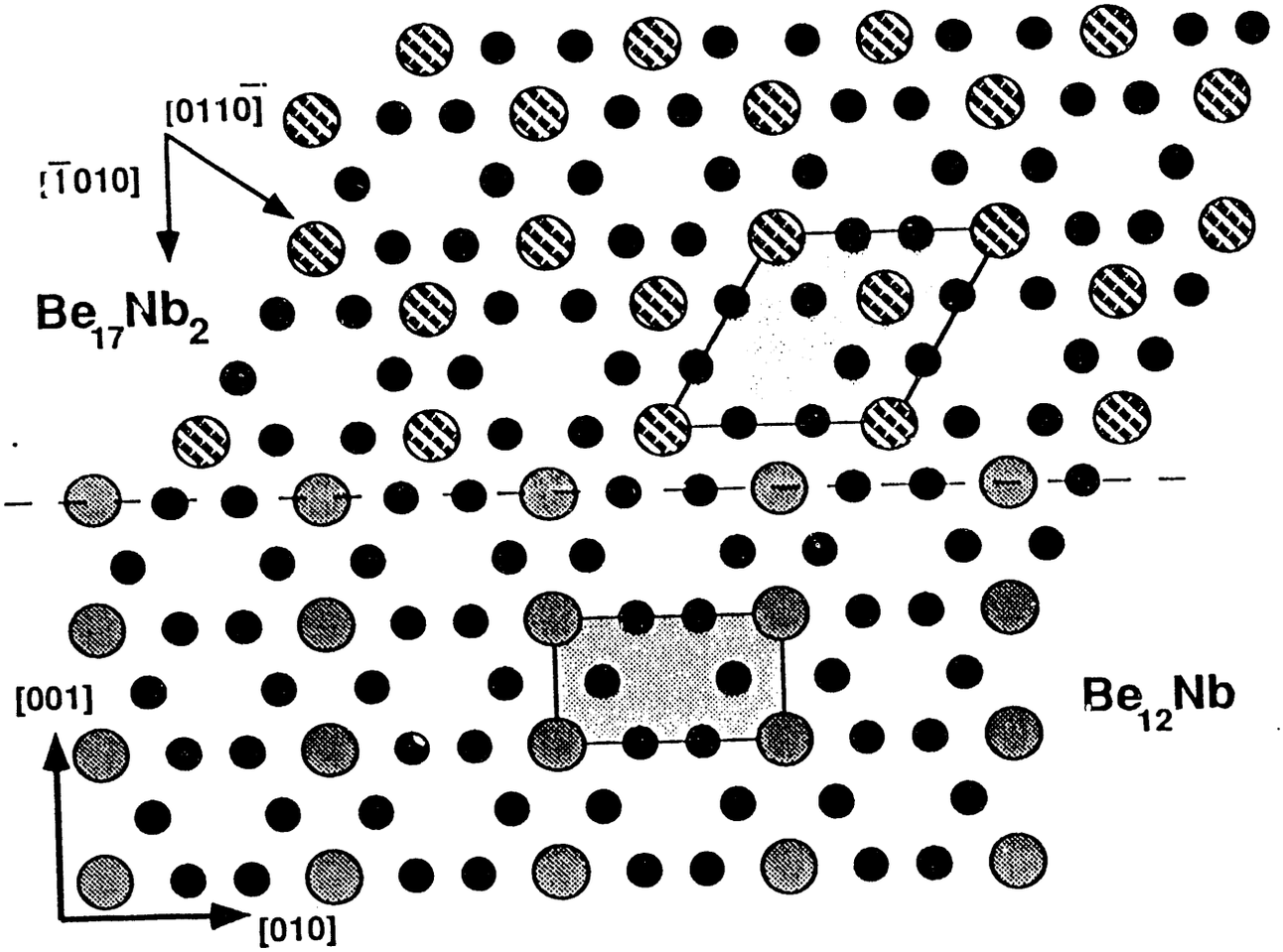

Figure 4. Illustration of the transformation from $Be_{12}Nb$ to $Be_{17}Nb_2$ by faulting on the (001) planes of the $Be_{12}Nb$ lattice.

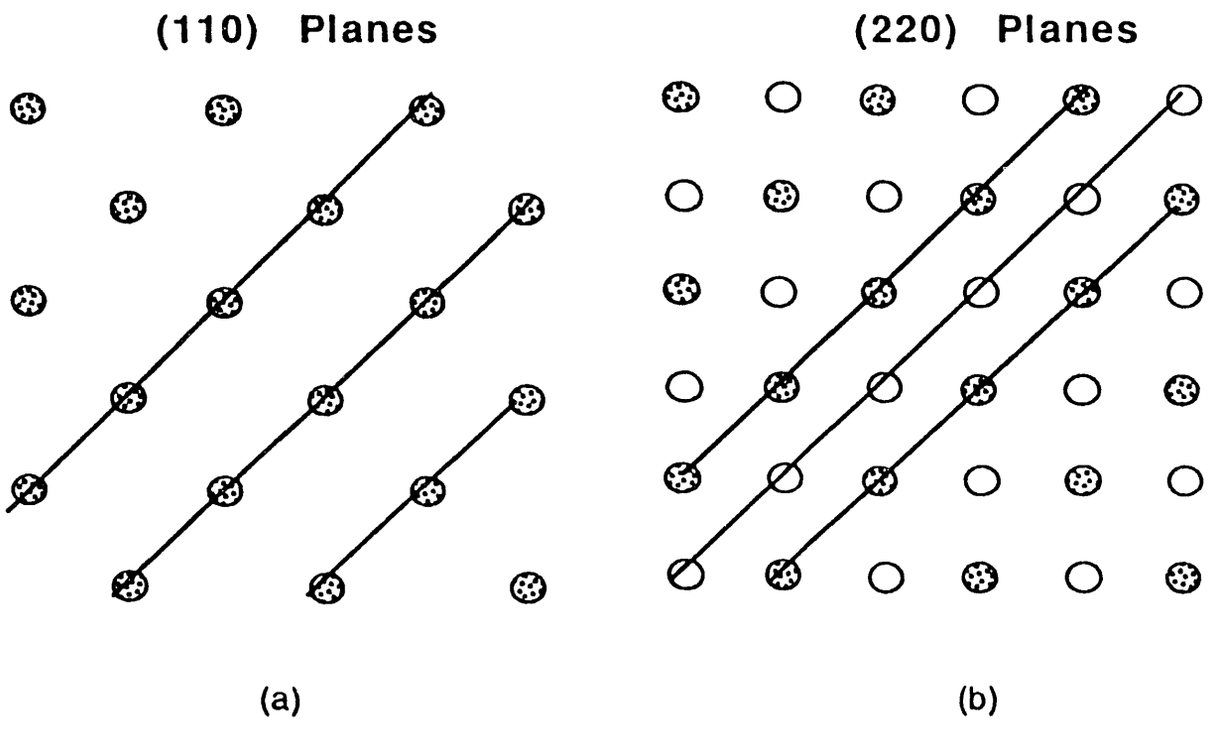

Figure 5. (a) (001) projection of the intersection of (110) planes in a perfect $Be_{12}Nb$ lattice. (b) Intersection of the same planes in a heavily faulted lattice. Vacant circles in (b) are atoms in the faulted position.

END

DATE
FILMED
12/16/91